X-662-71-304
PREPRINT

65654

SAS-B DIGITIZED SPARK CHAMBER GAMMA RAY TELESCOPE

S. M. DERDEYN
C. H. EHRMANN
C. E. FICHTEL
D. A. KNIFFEN
R. W. ROSS

AUGUST 1971

GSFC
GODDARD SPACE FLIGHT CENTER
GREENBELT, MARYLAND

SAS-B DIGITIZED SPARK CHAMBER GAMMA RAY TELESCOPE

S. M. Derdeyn, C. H. Ehrmann, C. E. Fichtel,
D. A. Kniffen, and R. W. Ross

NASA/Goddard Space Flight Center
Greenbelt, Maryland, U. S. A.

1. Introduction

The SAS-B gamma ray telescope represents the first satellite version of a planned evolution of gamma ray digitized spark chamber telescopes at Goddard which began with the development of a balloon-borne instrument. The heart of the telescope is a multilayer digitized spark chamber which can clearly establish a gamma ray event and reject events which, in other simpler instruments, might be indistinguishable from ones formed by gamma rays. The telescope is aimed at the study of gamma rays whose energy exceeds about 20 MeV.

In the early 1960's, it was realized that the celestial gamma ray intensity was very low compared to the high background of cosmic ray particles and earth albedo. For this reason, a picture type detector was needed to identify unambiguously the electron pair produced by the gamma ray and to study its properties--particularly to obtain a measure of the energy and arrival direction of the gamma ray. In addition, the secondary gamma ray flux produced by cosmic rays in the atmosphere severly limits the gamma ray astronomy which can ever be accomplished with balloons, and dictates that gamma ray astronomy must ultimately be pursued with detector systems on satellites. The combination of the need to develop

a satellite instrument together with the requirement of handling a large amount of data led to the development of a satellite-qualifiable magnetic core digitized spark chamber which provides data in a form suitable for telemetry and subsequent automatic analysis. Further, it was realized in 1963 when this research began that a digitized spark chamber could be used for many other experiments. A balloon version of the gamma ray instrument, which has been described earlier (Ehrmann, Fichtel, Kniffen, and Ross, 1967), was flown successfully on 10 million cubic foot balloons in 1966. A more complete discussion of the reasons for the choice of this type of picture detector is given in the article by Ehrmann et al. (1967).

2. General Description of the Instrument

A schematic diagram of the gamma ray telescope to be flown on the SAS-B satellite is shown in Fig. 1. The spark chamber assembly consists of 16 spark chamber modules above a set of four central plastic scintillators and another 16 modules below these scintillators. Thin tungsten plates, averaging 0.010 cm thick--corresponding to 0.03 radiation lengths---are interleaved between the spark chamber modules. In the upper half of the spark chamber assembly, these plates serve a dual purpose, first to provide material for the gamma ray to be converted into an electron pair and secondly to provide a means of determining the energy of the electrons in the pair. An estimate of the energy of each electron is obtained by measuring the average Coulomb scattering as they pass through the plates in the upper and lower spark chamber assemblies. The plates in the lower half of the spark chamber assembly are included primarily for the latter purpose.

The spark chamber assembly is normally triggered if a charged particle passes through one of the four square plastic scintillator tiles and the corresponding directional lucite Cerenkov counter immediately below, and, at the same time, there is no pulse in the surrounding plastic scintillator anticoincidence dome. Each of the four scintillator-Cerenkov counter telescopes acts independently of the others and has a full-width-half-maximum opening angle of about 30°. The anticoincidence dome prevents the spark chamber system from being triggered by charged particles, and the directional feature of the Cerenkov counter prevents the telescope from being triggered by upcoming neutral events or charged particles which might stop above the central scintillator before reaching the anticoincidence dome. An alternate trigger mode, which is described in the next section, is specifically aimed at detecting a very short pulse of high energy gamma rays of the type expected to be emitted during a supernova explosion. The effective area which is limited by the size of the Cerenkov scintillators is 540 cm^2. The opening angle for detection of gamma rays is approximately 1/4 Sr. The efficiency for detection of gamma rays of very high energy is 0.29, and for detection of 100 MeV gamma rays is about 0.21. The efficiency and solid angle as a function of energy will be determined precisely by calibration at the synchrotron facility of the National Bureau of Standards. Timing accuracy of better than two milliseconds, including transmission and ground station errors, is anticipated so that there can be a study of pulsed gamma ray sources.

By combining the energy and directional information for each electron in accordance with procedures described previously (Fichtel, Kniffen and Ogelman, 1969), the direction and energy of the primary gamma ray can be obtained. The uncertainty in the arrival direction for a gamma ray is about 1 1/2° at 100 MeV and varies with energy approximately as $E^{-2/3}$. The threshold is not sharp, but is about 20 to 25 MeV. The energy of the γ-ray can be measured up to about 200 MeV; above that energy the integral flux can be determined.

It is planned that SAS-B will be launched from San Marco off the coast of Kenya into an approximately circular orbit, with a 3° inclination and a 550 kilometer apogee. The satellite is capable of being pointed in any direction, but the time to change the direction of pointing is relatively long so that normally for the period of one orbit the satellite will point in essentially the same direction. Hence, for approximately 0.38 of the orbit the detector will point at the earth, and for another approximately 0.08 of the orbit the earth albedo gamma ray flux will be quite high, leaving about 0.54 of the orbit for collection of celestial gamma ray data. Combined with an expected percentage live time (the period when cores are not being read out and the gamma ray telescope is ready to accept another event) of about 90%, the portion of an orbit during which celestial data is collected is estimated to be just under 0.5. The net exposure for a one week viewing period directed at some point on the celestial sphere will be about $3.3 \times 10^7 cm^2 sec$ for 100 MeV gamma rays from a point source and about $10^7 cm^2 .sr.sec.$ for diffuse radiation.

3. Coincidence-Anticoincidence System

The spark chamber triggering telescopes consist of three parts - the centrally located scintillation counter array, the Cerenkov counters below the spark chambers, and the surrounding anticoincidence scintillator dome. The scintillation counter array is composed of four elements, each consisting of a 0.48 cm thick by 12.5 cm square piece of Pilot-M scintillator solvent bonded to an adiabatic acrylic light pipe which directs the optical signal through a pressure tight window in the bulkhead an RCA C7151Q photomultiplier outside the gas space. The four Cerenkov counters have an area of 135 cm^2 each and are 2.5 cm thick. They are made of UVT Plexiglas optically bonded to the face of a 12.7 cm diameter RCA C31029 stacked ceramic photomultiplier tube. The plastic blocks are painted with a highly absorptive coating on the upper surface to discriminate against upward moving charged particles. The anticoincidence dome is a highly polished single-piece casting of Pilot-B plastic scintillator material, measuring 66 cm inside diameter at the bottom, 56 cm high and averages 1.5 cm thick. The scintillator dome is viewed from the bottom edge by two groups of four equally spaced C7151Q photomultipliers whose outputs are summed to form the anticoincidence signal. Both groups of phototubes are normally operative and have an inefficiency of from 10^{-6} to 10^{-8} for the rejection of charged particles. In the event of a failure, either of the redundant groups would have a veto inefficiency of about 10^{-4}.

The coincidence system is shown schematically in Fig. 2. As can be seen, a spark chamber trigger pulse may be formed in one of two ways. The first, a two-fold coincidence, is generated whenever a charged particle passes through one of the four scintillator tiles and the Cerenkov counter directly beneath it. If this signal is not vetoed by a simultaneous pulse from the anticoincidence scintillator, the high voltage is applied to the spark chamber and the memory scan begun. The coincidence resolving time is 400 ns and the anticoincidence gate width is 600 ns. In addition to the spark chamber trigger pulse, a telescope flag pulse is routed to housekeeping to indicate which quadrant of the detector recorded the particle. This is done as an aid to the data processing. The spark chamber may also be triggered by the occurrence of the eight-fold coincidence of all four elements of both the scintillation counter and Cerenkov counter arrays. This technique is utilized for the detection of high intensity, short duration gamma-ray bursts such as might be associated with supernovae (Fichtel and Ogelman, 1968). A flag pulse is recorded in the housekeeping data to indicate this sort of trigger occurred.

In either mode of operation the spark chamber trigger is inhibited while the memory is busy transferring data. An additional inhibit may be generated, if allowed by ground command, when the charged particle rate at one of the scintillator tiles exceeds a few thousand per second.

The coincidence electronics are fabricated using conventional techniques of discrete and hybrid microelectronics, and incorporate considerable redundant circuitry. The electronic package weighs approximately 0.5 kg and use 500 mW of power.

4. Spark Chambers

The basic component of the spark chamber assembly is the wire grid spark module pictured in Fig. 3. This frame contains a 25 cm. by 25 cm. opening across which are strung two planes of 200 parallel and evenly spaced wires. The two planes are separated by 3.6 mm and the directions of the wires in these two planes are orthogonal. Each of the wires in a grid is terminated through a ferrite core which is set by the current which flows when the wire is associated with a spark. The manufacturing techniques used in the construction of these modules incorporate procedures established in the research and development program commencing in 1963; details of the development have been published previously (Ehrmann et al., 1967; O'Connor et al., 1968; Kniffen, 1969; and Ross et al., 1969).

The material chosen for construction of the module is glass bonded mica, selected for its low outgassing property, high dielectric strength, excellent dimensional stability, high modulus of elasticity, good structural yield strength, and ease of machining as compared to most ceramics. The frame design incorporates one piece construction and all unneeded material has been removed to meet critical weight constraints. The spark wires are made of 100 micron diameter beryllium copper. To maintain plane flatness they are attached under tension by ultrasonic welding and soldering

to copper pins embedded along the edges of the frame, and the plane to plane spacing is maintained to an accuracy of ±25 microns by machining the pin surfaces. Lateral placement of the wires within a plane is accomplished carefully locating the wire at the center of the pin with a ±25 microns tolerance. After attachment to the pins the wires are threaded through a ferrite core and attached to a common bus. The magnetic cores and additional components of the readout circuitry are mounted on shelves integral to the module material. This technique is used to provide additional structural rigidity to the frame as well as a low outgassing substrate for mounting electronic components. Printed circuit wiring is implemented by etching of a metal deposit on Kapton H-film bonded to the glass bonded mica shelf.

A module provides a two dimensional location for each spark through the cores set by the spark current flowing down a wire in one plane, through the spark, and onto a wire in the orthogonal plane. A third dimension to the picture is provided by the vertical stacking of the modules into two 16 module units, one above and one below the central scintillation level. The modules are interleaved with the 0.03 radiation length tungsten pair production and scattering plates. The entire assembly is attached to a cylindrical pedestal base which constitutes the primary structural member of the experiment.

Plane to plane separation in the spark module is made sufficiently large to yield a high probability of spark formation at one atmosphere of spark gas pressure, but no wider than necessary in order to minimize the applied voltage. These considerations led to the 3.6 mm gap width. Exten-

sive module tests were performed to optimize the performance of the spark chamber for the chosen gap width and gas pressure, with the additional requirement of at least one year satisfactory operation in space. Variables included in the study were: the gas composition, the applied voltage and the components in the high voltage pulser affecting the high voltage pulse shape. The gas composition chosen as a result of these tests contains 98.5 percent, by partial pressure, neon, 1.0 percent argon, to take advantage of the Penning (1940) effect and 0.5 percent ethanol, to suppress satellite sparkling. The performance characteristics observed for these parameters are shown in Fig. 4. Each module was tested to assure that its performance curves were satisfactory before incorporation into the spark chamber assembly.

The initial high voltage operating point was chosen such that the efficiency was on the plateau of the curve, but no higher than necessary so that the effects of spark spreading (the tendency for more than one wire to be read out for a single spark) would be minimized. As seen in Fig. 4, the initial operating point was chosen at about 2.5 Kv. In flight the operation will be monitored and shifts in the operating point due to gas aging or power supply drift will be compensated for by varying the adjustable high voltage supplies by commands to the satellite.

The high voltage pulsers, enclosed in two pressure tight boxes mounted alongside at the spark chamber stack, consist of 16 E.G. & G type KN-2 Krytron tubes, each discharging two separate energy storage capacitors onto individual spark chamber modules. The tubes are operated with a nominal anode potential of 2500 volts, a "keep-alive" current of 20 μamps,

and a trigger voltage of one kilovolt. Laboratory tests indicate the lifetime of the high voltage pulser to be above 10^7 pulses in this configuration. For redundancy, there are two completely separate systems, one connected to the odd numbered spark chamber modules and the other to the even numbered modules. If either system fails completely, every other spark chamber module will still be active.

5. Core Memory Readout System

A total of 12,800 cores are associated with the entire gamma ray spark chamber assembly. When the high voltage pulse is applied for an event, cores attached to those wires carrying spark current will be set. It is then necessary to determine the locations of the set cores and reset them before another event is accepted. From the standpoint of core readout, the entire spark chamber assembly is divided into two electrically isolated interleaved memories of 16 modules each. Each of the modules has two decks with 200 cores per deck to service the two orthogonal planes. The cores are read eight at a time by pulsing one of twenty-five current sources attached to the drive wires on each deck and the appropriate current sink, as shown in Figs. 5 and 6. Set cores are detected by eight sense amplifiers which are transformer coupled to the series connected sense lines in each chamber. Set cores are stored in an 8 bit shift register associated with each half of the spark chamber assembly.

A sequential scan of the core memory is initiated by a trigger pulse from the coincidence logic. When a set core is found, three

adjacent cores are examined. The number of adjacent set cores and the unique core sequence number of the last core are transferred to the telemetry interface system. This technique of core readout is adopted to reduce the number of bits required to record an event. During the readout operation a busy signal is provided to the coincidence logic to inhibit further triggers.

The telemetry interface system accepts 16 bits of information for each set core, or adjacent group of cores. 14 bits are allocated to a unique sequence number for each of the 12,800 cores, and 2 bits to denote up to four adjacent cores. The data are shifted into a storage register from which they are serially entered into the telemetry bit stream.

6. Housekeeping Data System

This sub-system accepts rate outputs from the various coincidence counter and logic gates. Included are the anticoincidence rate, commutated rates from the four central scintillators, rates from the four Cerenkov counters, coincidence rates from the four trigger telescopes and total trigger rate. It provides scalers for the measurement of these rates, with quasilogarithmic prescalers to extend the dynamic range of the scintillation counters to fit within the 8 bits allocated for housekeeping data words. Also recorded are five trigger mode flags to indicate which of the four charged particle telescopes triggered the event, if one of them did, or to indicate that the event was triggered by the supernova hodescope mode.

There are two time scalers which count gated spacecraft clock pulses to provide relative vernier time of event occurrence accurate, to better than one millisecond, and detector livetime information. When other

uncertainties are included, such as ground station clock errors, the occurrence of an event should be known in absolute time to better than two milliseconds. The contents of all scalers and storage registers are transferred in parallel to a buffer storage register and are transferred serially to the spacecraft telemetry system (Fig. 7).

7. Command System

The data command decoder accepts an enable gate, a 24 bit coded command instruction, and a command execute signal. The command is implemented by transmitting a coded bit string to the satellite where it is entered serially into an acceptance register from which it is transferred to an execute register by the execute signal. Proper reception of the command is verified through spacecraft telemetry. The coded commands provide for a series of engineering tests to examine experiment and readout system performance and to isolate possible experiment malfunctions. Also included is a previously discussed adjustment of the high voltage applied to the spark chambers to compensate for shifts in the operating point (Fig. 4) as the gas ages. A command system block diagram is given in Fig. 8.

8. Data Processing and Reduction

The data obtained in orbit are stored at a one kilobit per second rate on magnetic tape. Once per orbit, the tape recorder will be commanded into a playback mode to transmit the information accumulated for that orbit to a ground receiving station. The receiving station at Quito,

Ecuador is the prime one for data reception. The data from three orbits per day will be transmitted to the Goddard Space Flight Center for processing within 24 hours to determine spacecraft attitude and to monitor the experiment's performance. The experiment data from these orbits will be combined with the remaining data when it is processed to study the celestial gamma radiation in detail.

The spark chamber information will be analyzed using advanced versions of automatic computer techniques developed over the last several years to analyze balloon experiment data (Fichtel et al., 1971). The computer programs will examine all spark chamber telescope events. Each event classified as a gamma ray will be examined in detail to determine the energy and arrival direction of the photon. Spacecraft attitude and orbit data will be coupled with the event analysis to determine the celestial arrival direction of each gamma ray.

Events which cannot be analyzed automatically will be transferred to a Graphics Display Unit where a data analyst will examine the event and make necessary decisions to allow the automatic analysis to proceed. The display will also be used to analyze a selected number of "good" events to check the performance of the automatic procedure.

The final result of the analysis procedures outlined above will be to produce a master catalog of all observed gamma rays with a complete tabulation of their properties. The catalog will be accessible in manner sufficiently flexible to allow any aspect of the data to readily be retrieved for interpretation. In the same manner all engineering data will be accessible to monitor experiment performance.

FIGURE CAPTIONS

Fig. 1. A schematic diagram of the SAS-B digitized spark chamber gamma ray telescope.

Fig. 2. A coincidence system flow diagram. A refers to the anti-coincidence counter, B_i represents one of the four scintillation detectors and C_i the corresponding Cerenkov detector.

Fig. 3. A picture of one of the 32 wire grid modules contained in the SAS-B spark chamber.

Fig. 4. A graph of typical spark module performance characteristics.

Fig. 5. SAS-B spark chamber x and y core array.

Fig. 6. A block diagram of the SAS-B spark chamber core memory readout system.

Fig. 7. SAS-B housekeeping system block diagram.

Fig. 8. SAS-B command system block diagram.

REFERENCES

C. H. Ehrmann, C. E. Fichtel, D. A. Kniffen, and R. W. Ross, Nucl. Instr. and Meth. 56 (1967) 109.

C. E. Fichtel, D. A. Kniffen and H. B. Ogelman, Ap. J. 158 (1969) 193.

J. W. O'Connor, E. H. Pessagno and J. G. Etzel, GSFC Preprint X-284-68-278. (1968).

D. A. Kniffen, NASA Tech. Report TR R-308 (1969).

R. W. Ross, C. H. Ehrmann, C. E. Fichtel, D. A. Kniffen and H. B. Ogelman, IEEE Trans. Nuc. Sci. NS-16 (1969) 304.

M. J. Druyvestein and F. M. Penning, Rev. Mod. Phys. 12 (1940) 87.

C. E. Fichtel, R. C. Hartman, D. A. Kniffen and M. Sommer, GSFC Preprint X-662-71-209 (1971), submitted for publication to the Astrophysical Journal.

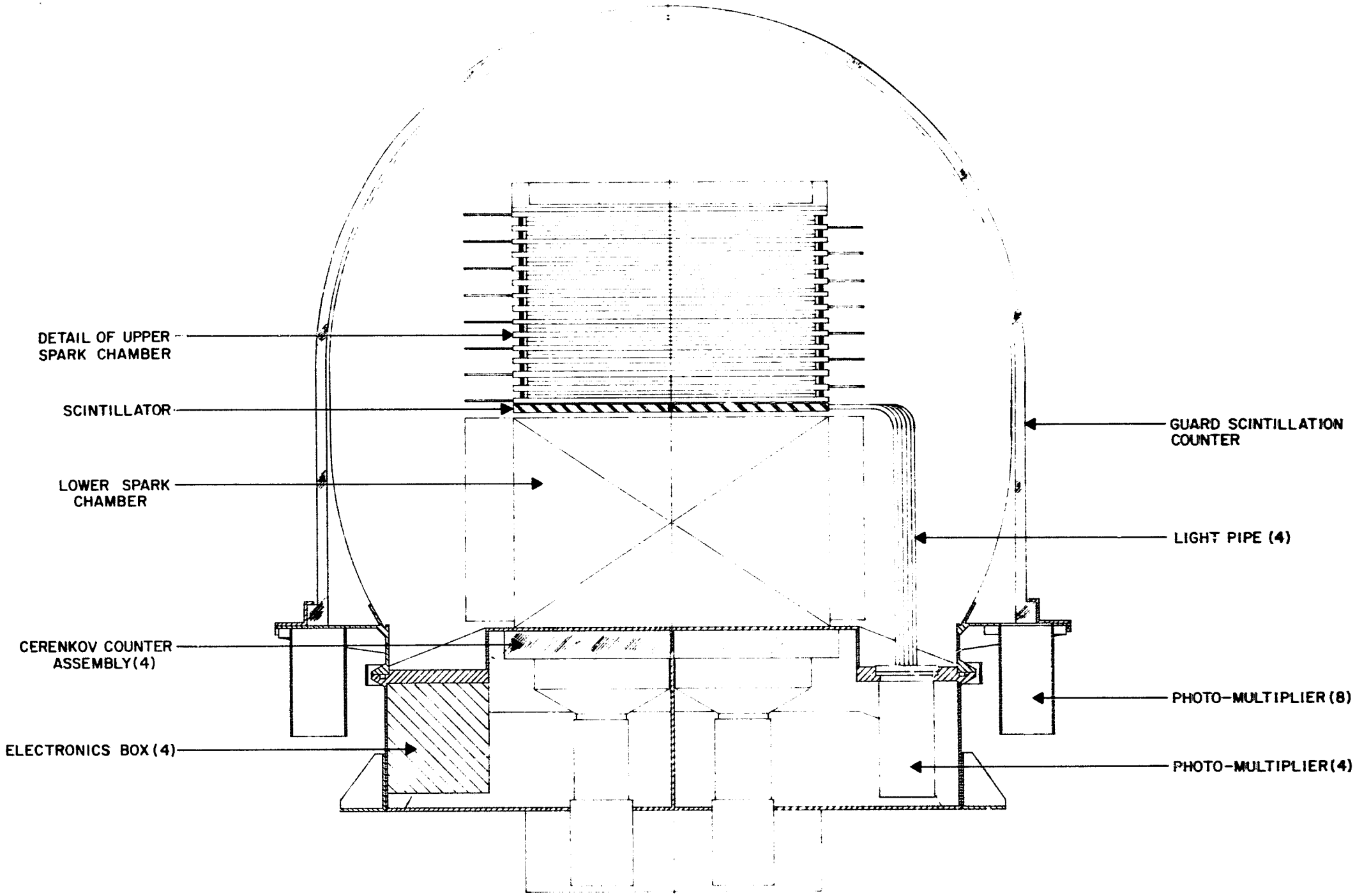

SAS-B GAMMA RAY EXPERIMENT

FIG. 1

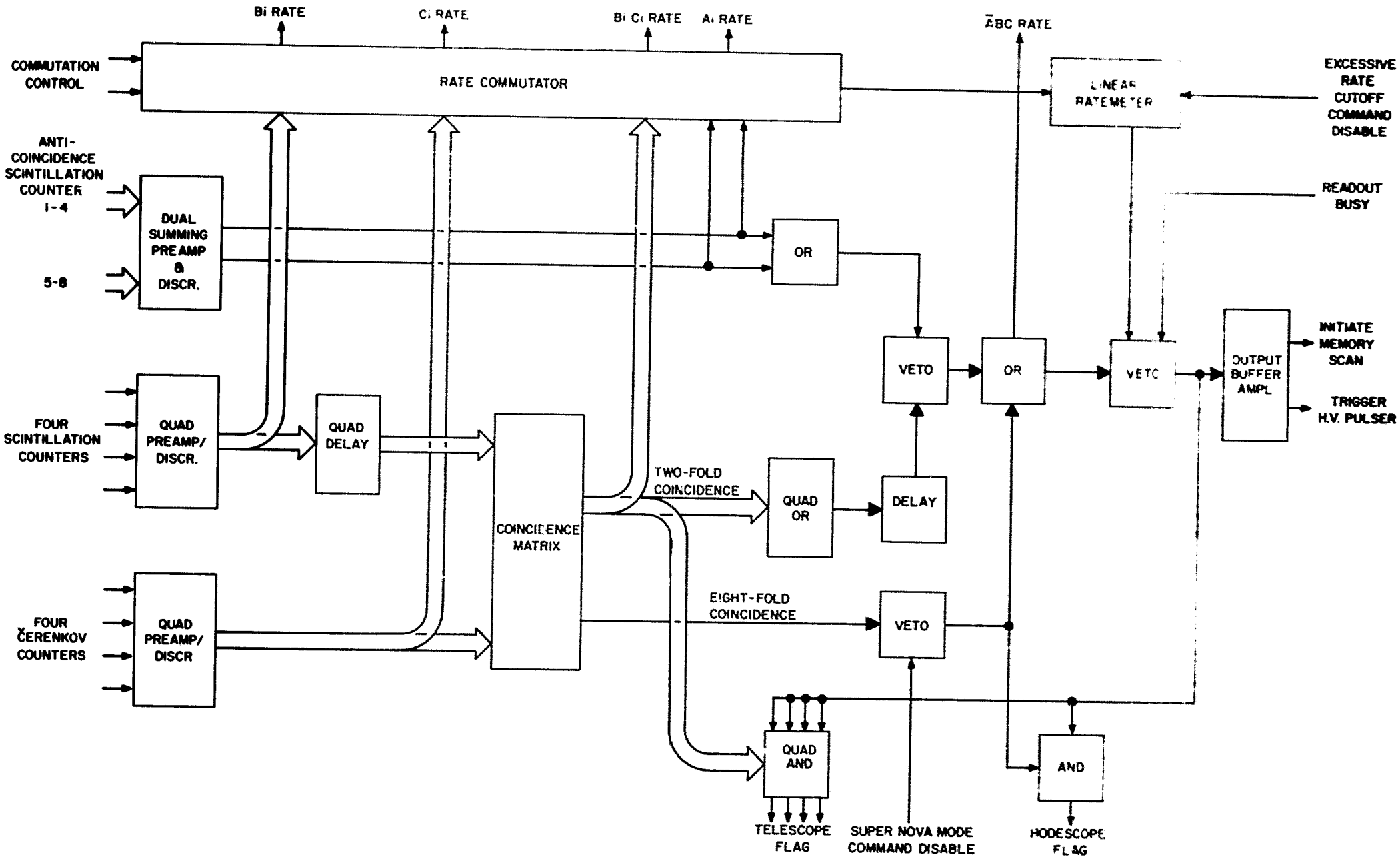
Bi RATE
Ci RATE
Bi Ci RATE
Ai RATE
ĀBC RATE
COMMUTATION CONTROL
RATE COMMUTATOR
LINEAR RATEMETER
EXCESSIVE RATE CUTOFF COMMAND DISABLE
READOUT BUSY
ANTI-COINCIDENCE SCINTILLATION COUNTER 1-4
5-8
DUAL SUMMING PREAMP & DISCR.
OR
VETO
OR
VETO
OUTPUT BUFFER AMPL
INITIATE MEMORY SCAN
TRIGGER H.V. PULSER
FOUR SCINTILLATION COUNTERS
QUAD PREAMP/ DISCR.
QUAD DELAY
COINCIDENCE MATRIX
TWO-FOLD COINCIDENCE
QUAD OR
DELAY
FOUR ČERENKOV COUNTERS
QUAD PREAMP/ DISCR
EIGHT-FOLD COINCIDENCE
VETO
QUAD AND
AND
TELESCOPE FLAG
SUPER NOVA MODE COMMAND DISABLE
HODESCOPE FLAG

FIG. 2

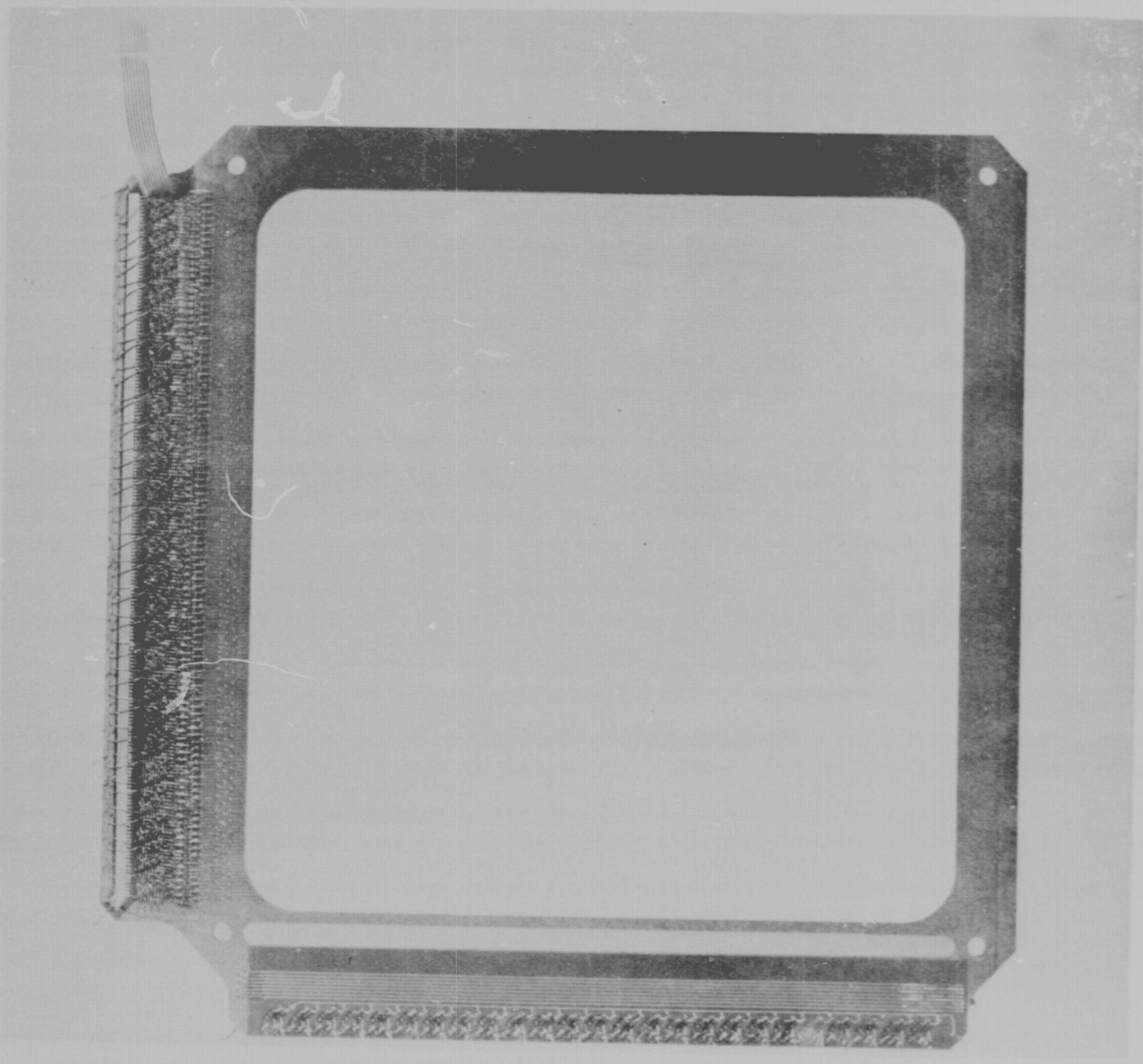

FIG. 3

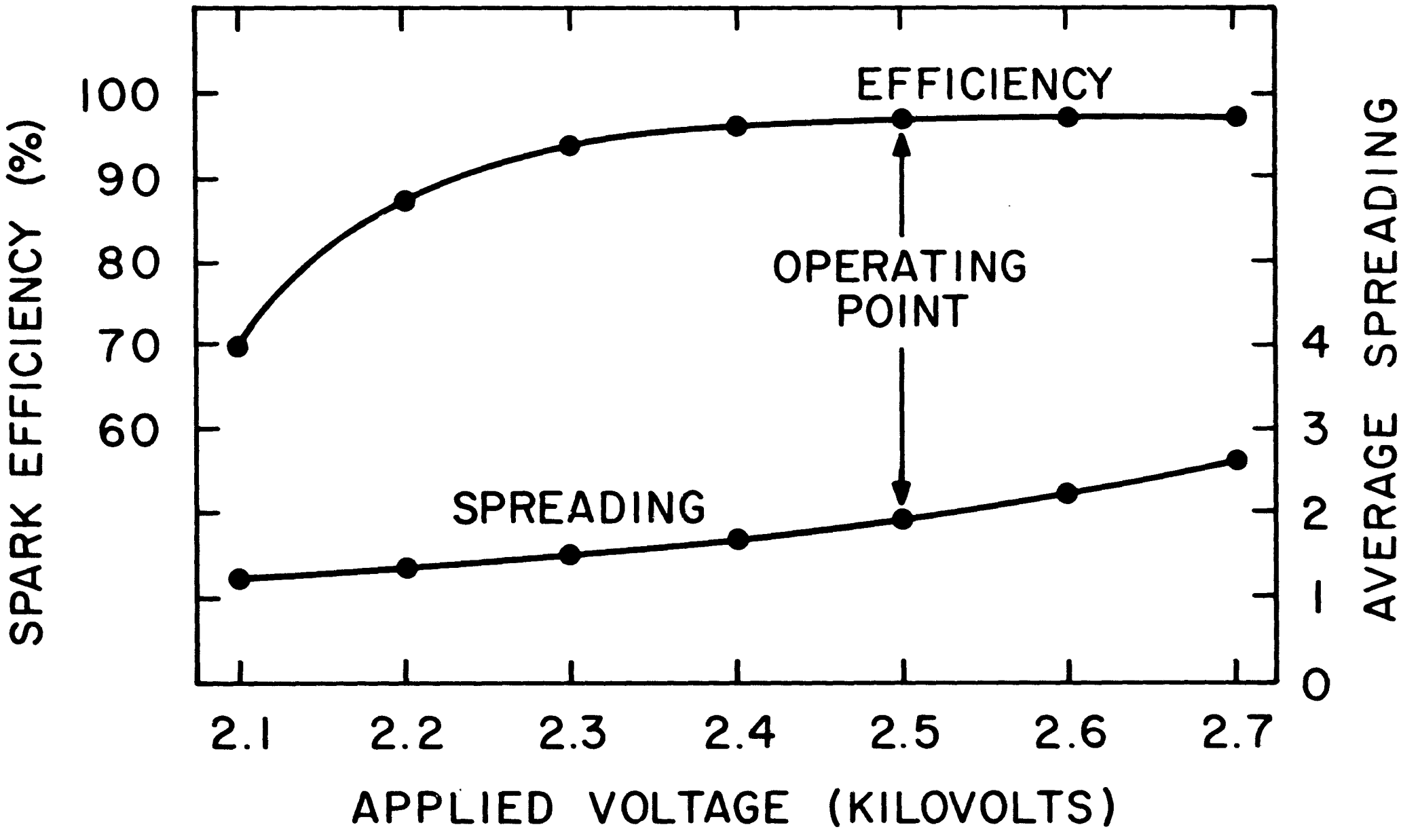
EFFICIENCY
OPERATING POINT
SPREADING
SPARK EFFICIENCY (%)
100
90
80
70
60
AVERAGE SPREADING
4
3
2
1
0
2.1
2.2
2.3
2.4
2.5
2.6
2.7
APPLIED VOLTAGE (KILOVOLTS)

FIG. 4

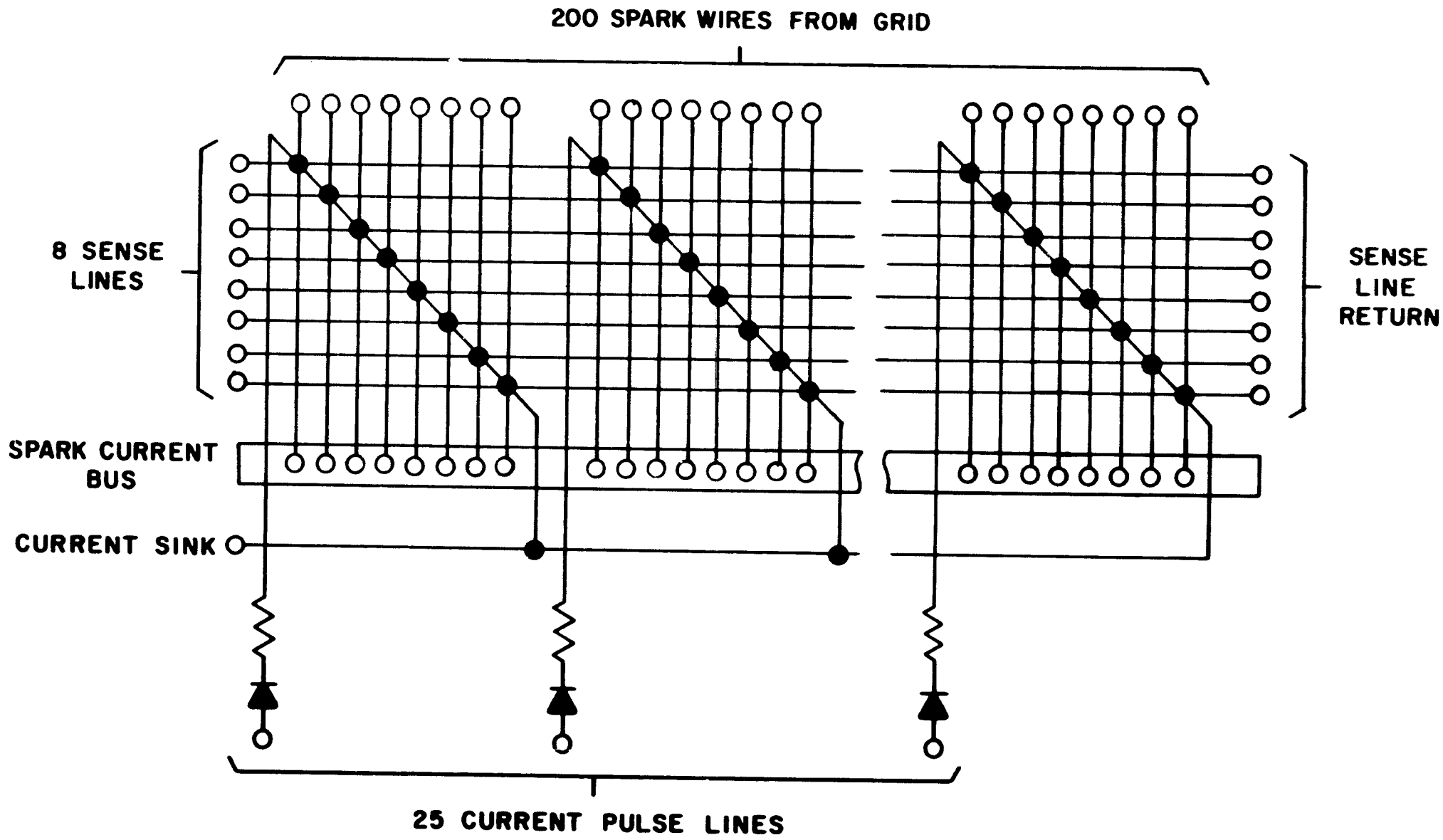

SAS-R SPARK CHAMBER X AND Y CORE ARRAY

FIG. 5

SAS-B SPARK CHAMBER BLOCK DIAGRAM

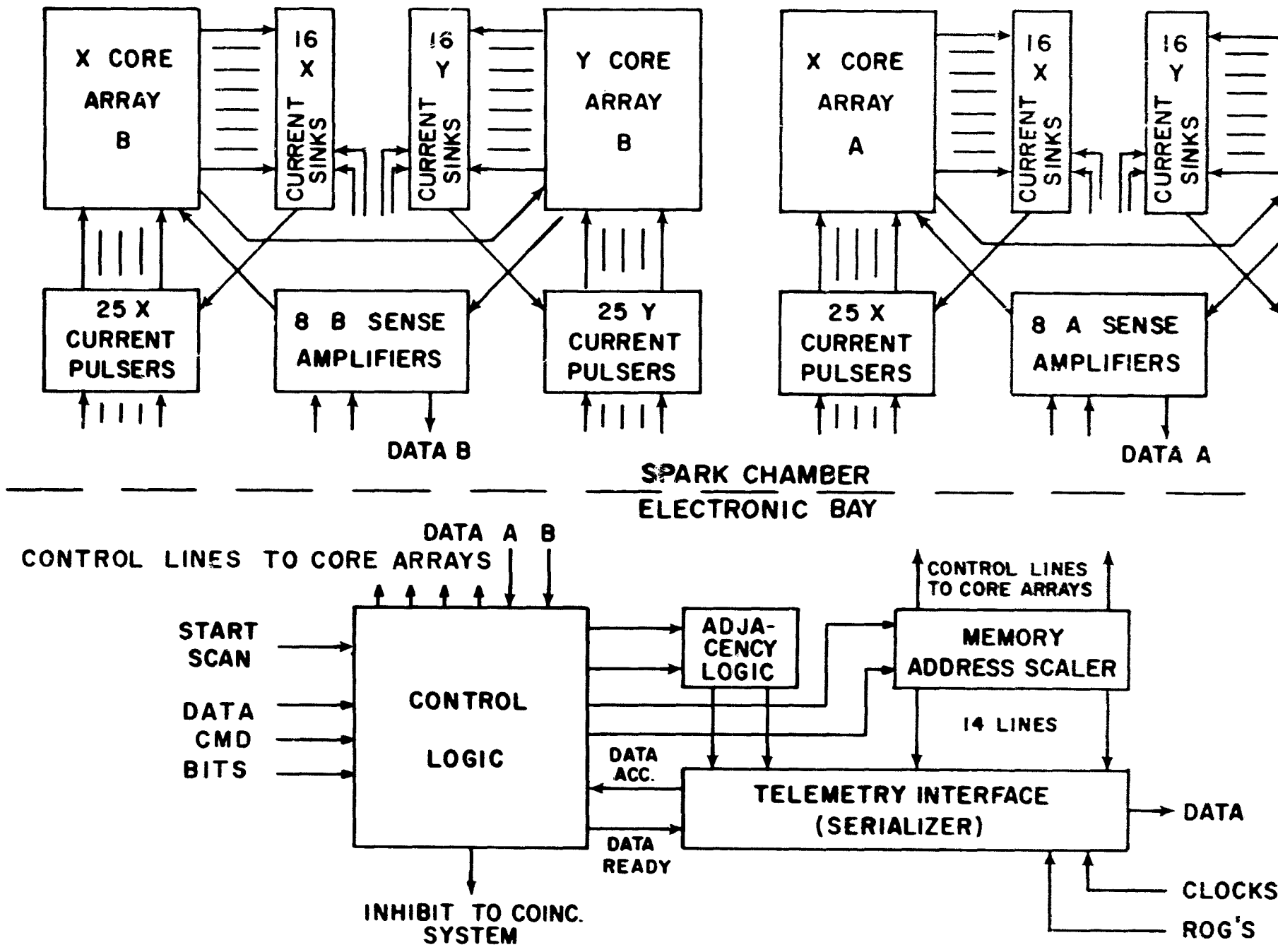

FIG. 6

SAS-B HOUSEKEEPING SYSTEM BLOCK DIAGRAM

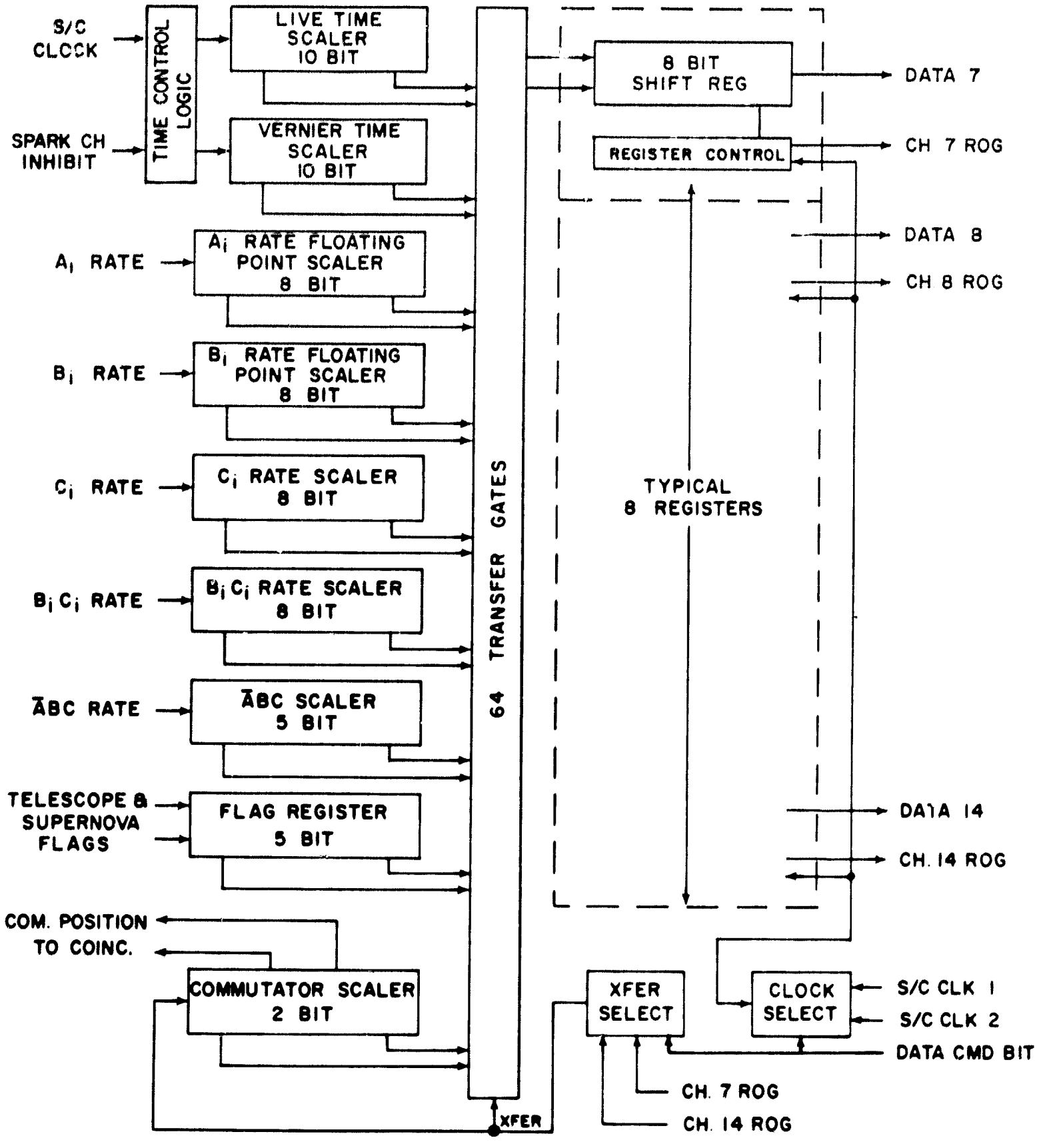

FIG. 7

SAS-B BLOCK DIAGRAM DATA COMMAND AND VERIFICATION SYSTEM

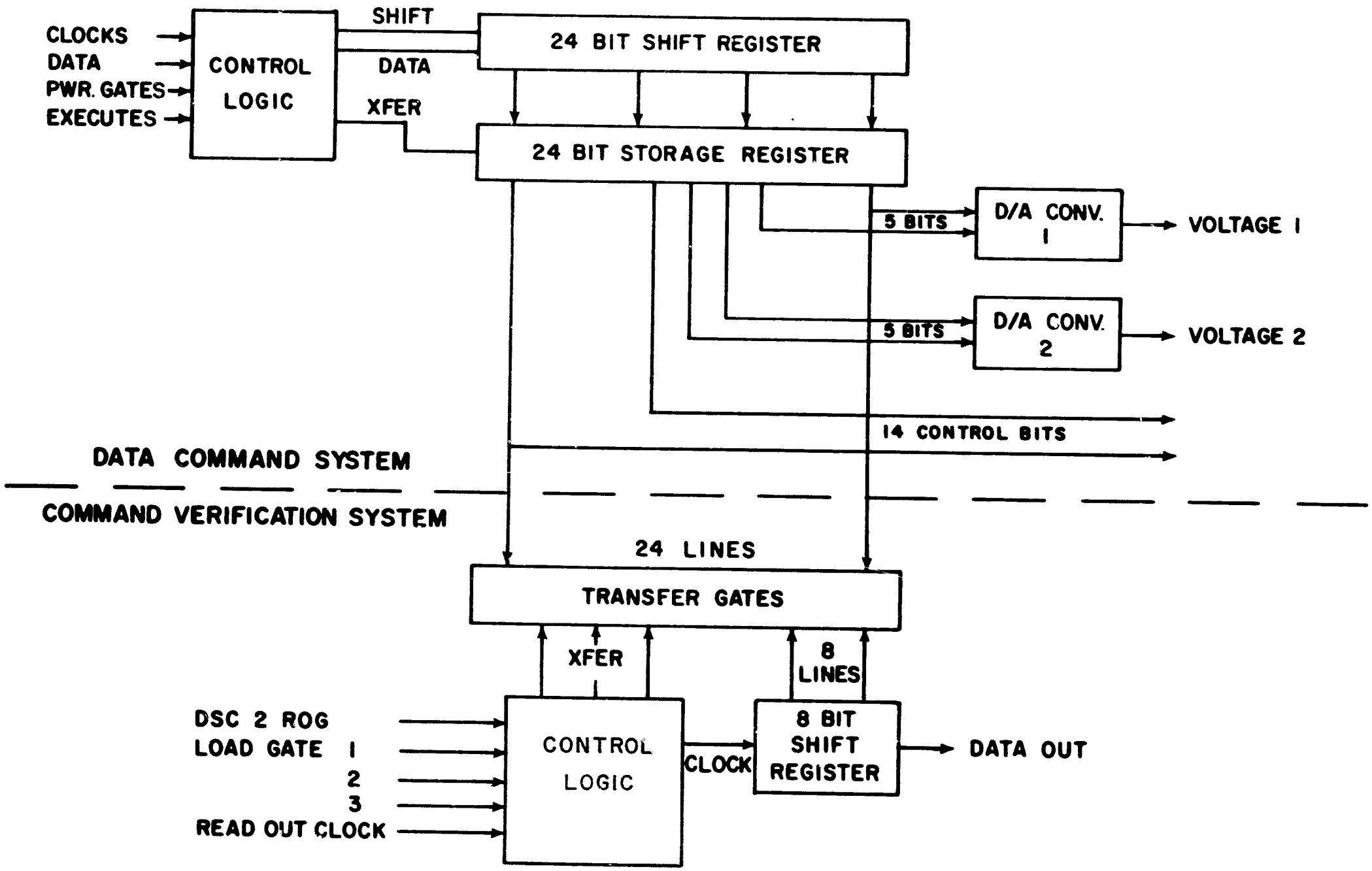

FIG. 8